THE JOURNAL OF PHYSICAL CHEMISTRY LETTERS
A JOURNAL OF THE AMERICAN CHEMICAL SOCIETY

pubs.acs.org/JPCL

Letter

Exciton Fine Structure in Axially Symmetric Quantum Dots and Rods of III−V and II−VI Semiconductors

Serguei V. Goupalov*

Cite This: J. Phys. Chem. Lett. 2024, 15, 11753−11759

Read Online

ACCESS | Metrics & More | Article Recommendations | Supporting Information

ABSTRACT: Both absorption and emission of light in semiconductor quantum dots occur through excitation or recombination of confined electron−hole pairs, or excitons, with tunable size-dependent resonant frequencies that are ideal for applications in various fields. Some of these applications require control over quantum dot shape uniformity, while for others, control over energy splittings among exciton states emitting light in different polarizations and/or between bright and dark exciton states is of key importance. These splittings, known as exciton fine structure, are very sensitive to the nanocrystal shape. Theoretically, nanocrystals of spheroidal shape are often considered, and their nonsphericity is treated perturbatively as stemming from a linear uniaxial deformation of a sphere. Here, we compare this treatment with a nonperturbative model of a cylindrical box, free of any restrictions on the cylinder's aspect ratio. This comparison allows one to understand the limits of validity of the traditional perturbative model and offers insights into the relative importance of various mechanisms controlling the exciton fine structure. These insights are relevant to both colloidal nanocrystals and epitaxial quantum dots of III−V and II−VI semiconductors.

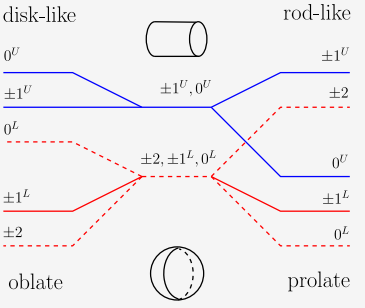

DARE TO COMPARE

Recent advances in single quantum dot spectroscopy[1] allow one to study the fine structure of excitons confined in colloidal nanocrystals with unprecedented precision. The exciton fine structure is very sensitive to the overall symmetry of a nanocrystal. When the symmetry of the nanocrystal shape is lower than that of the underlying crystal lattice, it will be revealed in the exciton fine structure.[2,3]

Within the effective-mass approximation, one often considers nanocrystals of spheroidal[1,4−8] or ellipsoidal[2,3,8,9] shape due to the efficiency of the method known as the perturbation theory of the boundary conditions, originally developed by A.B. Migdal[10,11] and, independently, by S.A. Moszkowski[12] to find energy levels of a deformed atomic nucleus. In this method, a spheroidal shape results from a uniform uniaxial deformation of a sphere preserving its volume. Performing a coordinate transformation, one can regain the spherically symmetric boundary condition at the expense of an anisotropic addition to the Hamiltonian, treated as a perturbation.

For a spheroid with semiaxes b and c, whose surface is described by the equation

$$\frac{x^2 + y^2}{b^2} + \frac{z^2}{c^2} = 1$$

the small parameter of Migdal's theory is

$$\mu_z = 2\frac{c - b}{c + b} \tag{1}$$

(in Migdal's book and Moszkowski's article the notations β and $3\,d/2$, respectively, are used for μ_z). The spheroid's aspect ratio is related to μ_z through

$$\frac{c}{b} = \frac{2 + \mu_z}{2 - \mu_z}$$

Migdal's theory is linear in μ_z and valid for $|\mu_z| \ll 1$.

In this work we will compare this treatment with a nonperturbative model of cylindrical nanorods, free of any restrictions on the cylinder's aspect ratio. This comparison will allow one to understand the limits of validity of the approach based on Migdal's theory, and offer insights into relative importance of various mechanisms controlling the exciton fine structure in nanocrystals.

In what follows, we will consider the ground exciton state in a zincblende nanocrystal of a III−V or II−VI semiconductor formed by the hole from the valence band Γ_8 and the electron from the conduction band Γ_6. For simplicity, we will neglect the spin−orbit split-off valence band whose role is discussed in refs.[8,13] For a nanocrystal of spheroidal shape, the linear in μ_z perturbation splits the ground level of the confined hole, characterized by the hole total angular momentum 3/2,[14] into

Received: October 4, 2024
Revised: November 13, 2024
Accepted: November 14, 2024

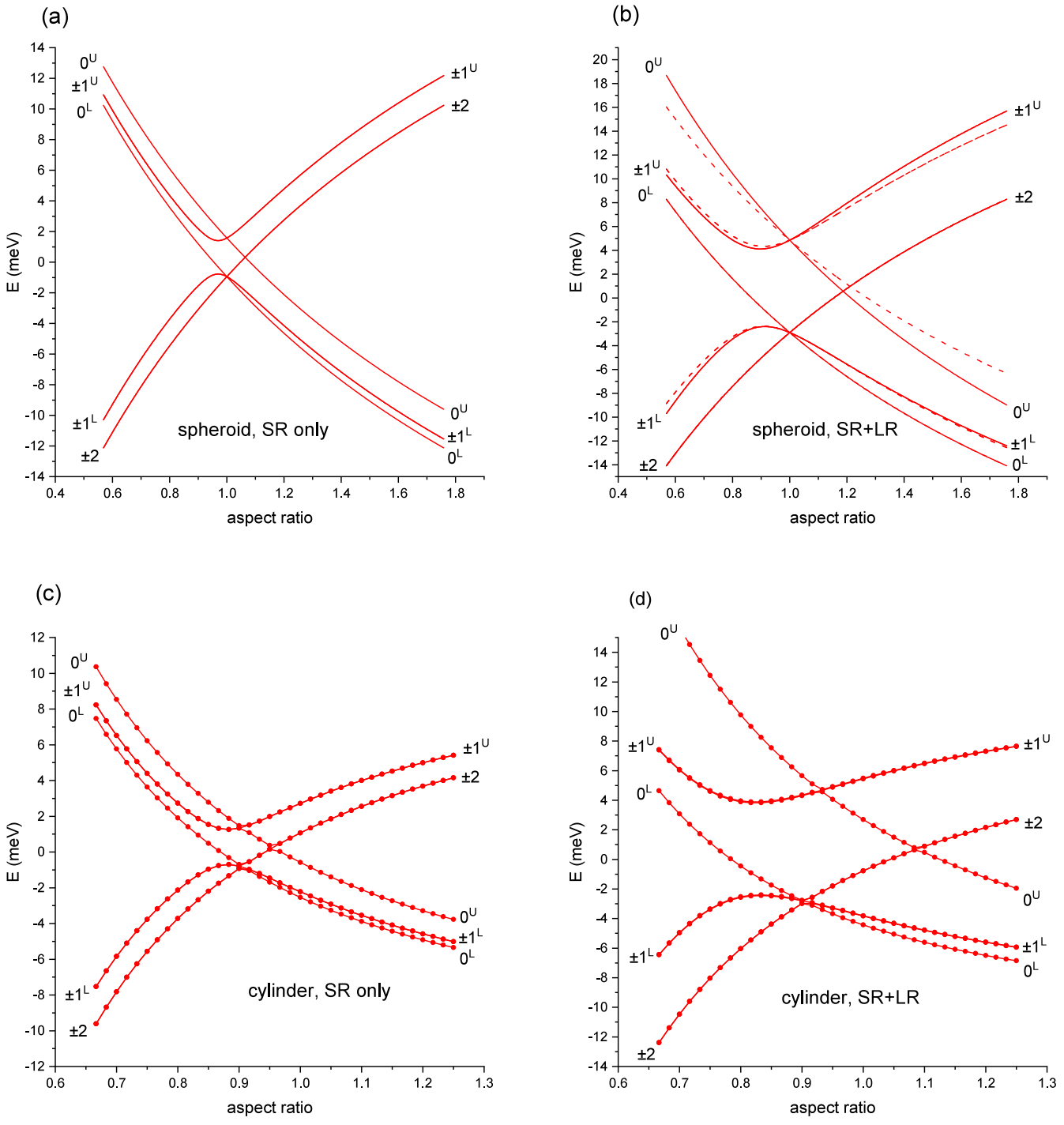

Figure 1. (a) Fine structure of the ground exciton multiplet in a spheroidal zincblende CdSe nanocrystal obtained from a uniform uniaxial deformation of a sphere of radius R = 30 Å, shown as a function of the spheroid aspect ratio and calculated taking into account only the short-range part of the electron−hole exchange interaction. (b) Same as (a), but calculated taking into account the isotropic part of the electron−hole long-range exchange interaction and neglecting (dashed lines) and taking into account (solid lines) its anisotropic part. (c) Energy levels of the 8 lowest exciton states in a zincblende CdSe cylindrical nanorod of radius R = 30 Å and height H shown relative to their average energy position as a function of the nanorod aspect ratio, $H/2R$, and calculated taking into account only the short-range part of the electron−hole exchange interaction. (d) Same as (c), but calculated taking into account both short-range and long-range parts of the electron−hole exchange interaction.

sublevels with the hole angular momentum projections onto the spheroidal axis of revolution equal to ±3/2 and ±1/2, respectively. When combined with the isotropic part of the electron−hole exchange interaction, the effective spin-Hamiltonian, describing exciton fine structure, takes the form (see the Supporting Information for an explicit form of the matrix)

$$H = -\eta(\boldsymbol{\sigma}\mathbf{J}) - \frac{\mu_z \Delta_{sh}}{2}\left(J_z^2 - \frac{5}{4}\right) \quad (2)$$

where η is the exchange energy contributed by both the short-range and the long-range parts of the electron−hole exchange interaction,[15,16] J_α ($\alpha = x, y, z$) are the matrices of angular momentum j = 3/2, σ_α are the Pauli matrices, and Δ_{sh} is a

https://doi.org/10.1021/acs.jpclett.4c02800
J. Phys. Chem. Lett. 2024, 15, 11753−11759

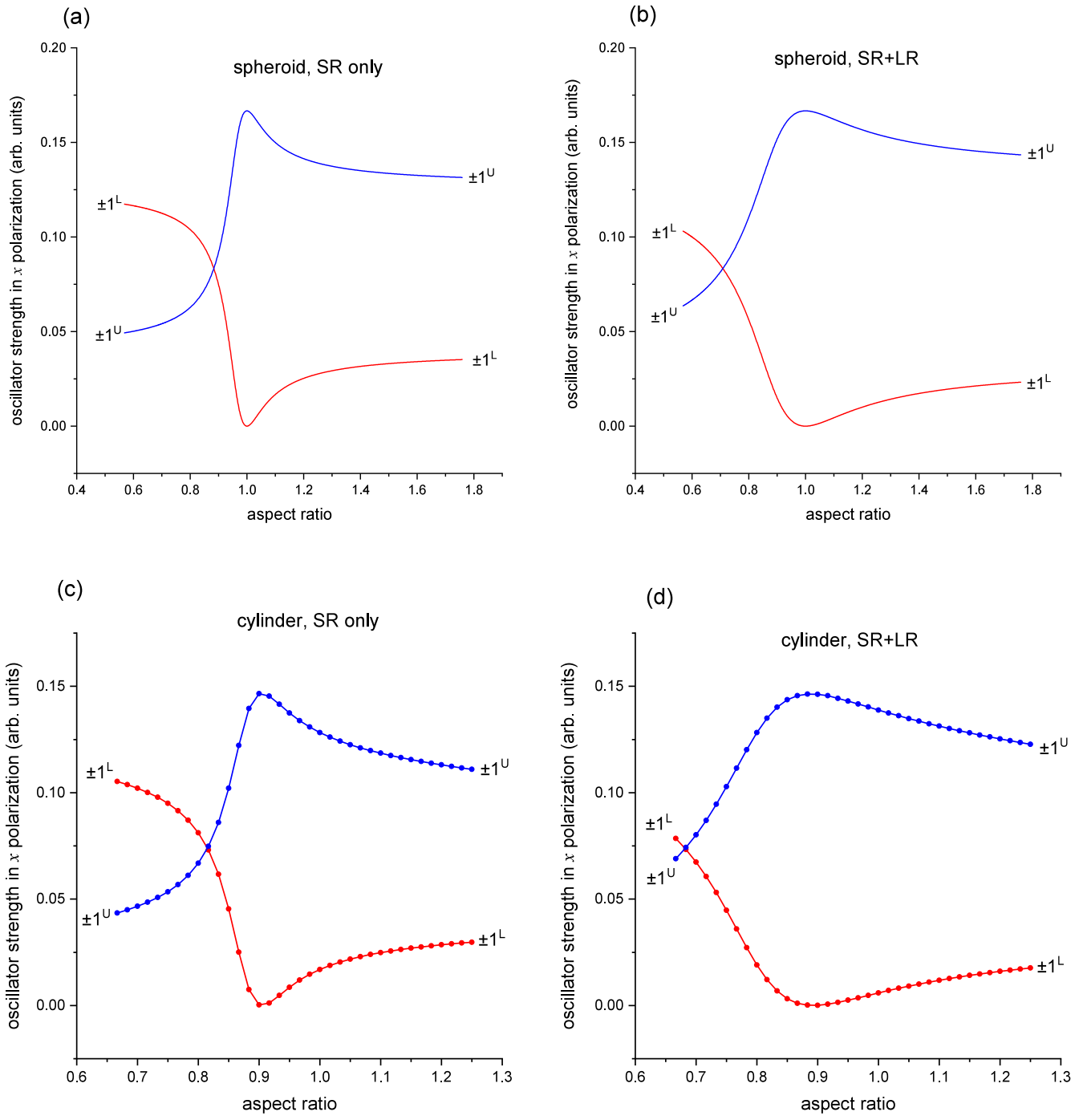

Figure 2. (a) Oscillator strengths for x-polarized optical transitions to the $\pm 1^L$ and $\pm 1^U$ exciton states in a spheroidal zincblende CdSe nanocrystal obtained from a uniform uniaxial deformation of a sphere of radius $R = 30$ Å, shown as functions of the spheroid aspect ratio and calculated taking into account only the short-range part of the electron−hole exchange interaction. (b) Same as (a) but calculated taking into account both short-range and long-range parts of the electron−hole exchange interaction. (c) Oscillator strengths for x-polarized optical transitions to the $\pm 1^L$ and $\pm 1^U$ exciton states in a zincblende CdSe cylindrical nanorod of radius $R = 30$ Å and height H, shown as functions of the nanorod aspect ratio, $H/2R$, and calculated taking into account only short-range part of the electron−hole exchange interaction. (d) Same as (c), but calculated taking into account both short-range and long-range parts of the electron−hole exchange interaction.

characteristic energy depending on material parameters (for CdSe $\Delta_{sh} < 0$).[8] While the exchange energy η scales as R^{-3} with the radius R of the deformed sphere, Δ_{sh} scales as R^{-2}.

In order to derive the second term in the right-hand side of eq 2, one has to apply the coordinate transformation $x \to x\, b/R \approx x\,(1-\mu_z/3), y \to y\, b/R \approx y\,(1-\mu_z/3), z \to z\, c/R \approx z\,(1+2\,\mu_z/3)$ [or, equivalently, $k_{x,y} \to k_{x,y}\,(1+\mu_z/3)$, $k_z \to k_z\,(1-2\,\mu_z/3)$] to the hole kinetic energy, given by the Luttinger Hamiltonian,[17] and evaluate matrix elements of the resulting perturbation on the multicomponent wave function of the hole confined in the sphere.[4,8]

Likewise, the long-range part of the electron−hole exchange interaction (or its Fourier transform) depends on the coordinates (wave vectors).[15,16] Therefore, a similar coordinate

https://doi.org/10.1021/acs.jpclett.4c02800
J. Phys. Chem. Lett. 2024, 15, 11753−11759

change in the framework of Migdal's theory, after evaluation of the corresponding matrix elements (this time on the exciton wave function), will result in a μ_z-dependent addition to the spin-Hamiltonian. This addition takes the form (see the Supporting Information for derivation and an explicit form of the matrix)

$$\Delta H = \mu_z \left\{ A\left(J_z^2 - \frac{5}{4}\right) + \frac{A + 2B}{3}\left[(\sigma_x V_x - \sigma_y V_y) + \sum_\alpha \sigma_\alpha J_\alpha^3 - 3\sigma_z J_z^3\right] - \frac{5A + 18B}{12}[(\boldsymbol{\sigma J}) - 3\sigma_z J_z]\right\} \quad (3)$$

where $V_x = J_x (J_y^2 - J_z^2) + (J_y^2 - J_z^2) J_x$, while V_y can be obtained by cyclic permutations of the indices. The coefficients A and B entering eq 3 can be expressed in terms of the dimensionless functions $I_0(y)$ and $I_2(y)$ known from the theory of the long-range electron−hole exchange interaction in excitons confined in nanocrystals[16]

$$A = \frac{\hbar\omega_{LT}}{2^3\pi^2}\left(\frac{a_B}{R}\right)^3 \int_0^\infty \mathrm{d}y\, y^2 \frac{I_0^2(y) - I_2^2(y)}{15}$$

$$B = \frac{\hbar\omega_{LT}}{2^3\pi^2}\left(\frac{a_B}{R}\right)^3 \int_0^\infty \mathrm{d}y\, y^2 \frac{I_0^2(y) + I_0(y)I_2(y)}{15}$$

where $\hbar\omega_{LT}$ is the longitudinal-transverse splitting of the exciton polariton in the bulk and a_B is the bulk exciton Bohr radius.

The ground exciton state in a spheroidal nanocrystal is formed by a hole with the total angular momentum projections $\pm 3/2, \pm 1/2$ and an electron with spin projections $\pm 1/2$. For a sphere with $\mu_z = 0$ and the aspect ratio $c/b = 1$, both the second term in the right-hand side of eq 2 and the anisotropic correction (3) are zeros, while the isotropic exchange interaction splits the exciton state into a bright triplet with the exciton total angular momentum 1 and a dark 5-fold degenerate state with the exciton total angular momentum 2. When $\mu_z \neq 0$, the exciton total angular momentum is no longer a good quantum number, unlike the absolute values of its projections onto the axis z, which can still be used to characterize the exciton states in a nanocrystal with an axially symmetric shape. The second term in the right-hand side of eq 2 lowers (raises) the $M = \pm 3/2$ hole level with respect to that with $M = \pm 1/2$ when $\mu_z < 0$ ($\mu_z > 0$), leading to changes in the exciton fine structure. This is illustrated in Figure 1, (a), (b), where the energy levels of a spheroidal zincblende CdSe nanocrystal are shown as functions of the spheroid's aspect ratio when only the short-range electron−hole exchange contribution to the parameter η is taken into account (Figure 1, (a)), and when both the short-range and the long-range parts of the electron−hole exchange interaction are accounted for (Figure 1, (b)). In the latter case, dashed (solid) lines show energy levels calculated neglecting (taking into account) the contribution of eq 3. As expected,[18] when it is taken into account, the exciton states, strongly polarized along the axis of revolution (0^U) and in the plane perpendicular to it ($\pm 1^U$), effectively repel one another, when the anisotropy increases.

For simplicity, in our calculations we neglected the difference in dielectric permittivities of the nanocrystal and its environment affecting the long-range electron−hole exchange contribution.[16]

One of the advantages of the effective-mass approximation is that it allows one to predict the properties of nanostructures based on the parameters which can be obtained from the measurements on bulk materials. However, while zincblende CdSe nanocrystals can be synthesized along with their wurtzite counterparts, bulk CdSe only crystallizes as wurtzite. Fortunately, within the effective-mass approximation, the electronic structure of the wurtzite crystal can be obtained from its zincblende counterpart, introducing the crystal field which splits the hole energy dispersion in a zincblende crystal, degenerate at the Γ point of the Brillouin zone, into subbands of the light and heavy holes. Thus, one can describe the zincblende CdSe by taking the parameters of wurtzite CdSe and setting the crystal-field splitting equal to zero. These parameters are known from the experimental investigation of the exciton polariton dispersion in bulk CdSe.[19] The values of the parameters used in our calculations can also be found in ref.[16]

While electron−hole exchange interaction splits the exciton state of a sphere ($\mu_z = 0$, aspect ratio $c/b = 1$) into a radiative triplet and a 5-fold degenerate dark state, $\mu_z \neq 0$ induces mixing between the lower $\pm 1^L$ and upper $\pm 1^U$ exciton doublets, as illustrated in Figure 2, (a), (b) where we show oscillator strengths of the optical transitions linearly polarized in the x direction as functions of the aspect ratio.

Note, however, that Migdal's theory is not valid for significantly low or significantly high aspect ratios, and Figures 1, (a), (b) and 2, (a), (b) should be considered as extrapolations. Indeed, when $|\mu_z| = 0.32$ (aspect ratios of 1.38 or 0.72), $\mu_z^2 \approx 0.1$, and, strictly speaking, terms of higher orders in μ_z can no longer be neglected.

Thus, far, we have not mentioned the direct Coulomb interaction between the electron and the hole. As this interaction does not affect the spin degrees of freedom, in the regime of strong confinement of charge carriers it merely shifts the "center of gravity" of the excitonic multiplet without affecting its fine structure splittings.

Now let us consider a nanorod in the shape of a circular cylinder of radius R and height H. The states of a confined hole from the valence band Γ_8 can be written in the basis of four cylindrically symmetric wave functions of the form

$$\Psi_\nu^{M,n,n_z}(\rho, \varphi, z) = \frac{e^{i(M-\nu)\varphi}}{\sqrt{2\pi}}\sqrt{\frac{2}{H}}\sin\frac{\pi n_z z}{H} \times C_{M-\nu,n} J_{M-\nu}\left(x_{M-\nu,n}\frac{\rho}{R}\right)|\Gamma_8, \nu\rangle$$

Here, $|\Gamma_8,\nu\rangle$ is the Bloch function at the top of the valence band corresponding to the hole spin projection ν onto the cylindrical axis of the nanorod ($\nu = 3/2, 1/2, -1/2, -3/2$), $x_{L,n}$ is the n-th zero of the Bessel function, $J_L(x)$

$$C_{L,n} = \frac{\sqrt{2}}{R|J_{L+1}(x_{L,n})|}$$

is the normalization coefficient, and n, n_z, N, and N_z are natural numbers such that $1 \le n \le N$, $1 \le n_z \le N_z$. These four functions are characterized by the quantum number M, the projection of the hole total angular momentum onto the cylindrical axis, z, and they vanish on the surfaces of the nanostructure. Since these functions for different n and n_z are orthogonal, one can achieve higher numerical precision by taking into account more values for these indices.

One can calculate matrix elements of the Luttinger Hamiltonian[17] on these functions and perform numerical diagonalization of the resulting $4\,N\,N_z \times 4\,N\,N_z$ matrix. This yields single-particle energy levels of the confined hole for each particular value of the quantum number $|M|$. The four lowest

https://doi.org/10.1021/acs.jpclett.4c02800
J. Phys. Chem. Lett. 2024, 15, 11753−11759

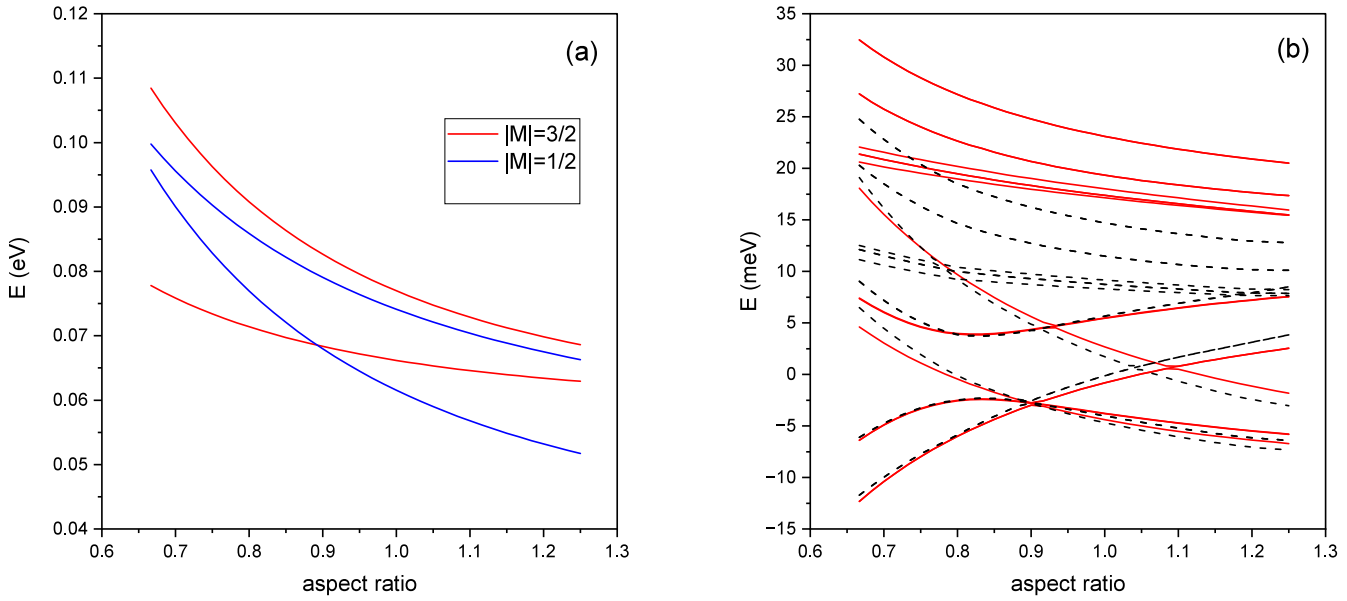

Figure 3. (a) Four lowest single-particle energy levels of a hole confined in a zincblende CdSe cylindrical nanorod of radius R = 30 Å and height H shown as a function of the nanorod aspect ratio, $H/2R$. The levels characterized by the hole total angular momentum projections M = ± 3/2 and M = ± 1/2 are shown by red and blue lines, respectively. (b) Same as Figure 1, (d) but with more energy levels shown. Also shown with black dashed lines are results obtained neglecting direct Coulomb interaction.

hole levels in a zincblende CdSe nanorod of the radius R = 30 Å are shown in Figure 3, (a) as functions of the rod's aspect ratio. The hole levels are characterized by the absolute values of the total hole angular momentum projections onto the rod's axis. One can see that the two lowest hole levels characterized, respectively, by $|M|$ = 3/2 ("heavy hole") and $|M|$ = 1/2 ("light hole"), are degenerate at the rod's aspect ratio close to 0.9. Unlike the case of a spheroidal nanocrystal, where this degeneracy corresponded to the case of the highly symmetric spherical shape, here this degeneracy is rather accidental.

The two lowest hole levels, out of the four shown in Figure 3, (a), are responsible for the fine structure of the lowest excitonic multiplet [cf. eq 2]. The fine structure results when we take into account the wave function of the confined electron and complement the system's Hamiltonian by the matrix elements of the electron−hole short-range and long-range exchange interactions. Since both the indices M and ν run through ±3/2, ± 1/2, once the electron spin is taken into account, the dimension of the matrix to be diagonalized becomes 32 $N N_z$ × 32 $N N_z$. As light-hole and heavy-hole excitons can have slightly different binding energies depending on the cylinder's aspect ratio, we also take into account the direct Coulomb interaction between the electron and the hole. The value of ε_0 = 9.6 is used for the static dielectric constant.[20] The resulting exciton fine structure is shown in Figures 1, (c), (d), neglecting and taking into account the long-range part of the electron−hole exchange interaction, respectively. The energy levels are shown with respect to the average energy positions of the eight lowest exciton states, calculated at each aspect ratio. Although it is no longer required by the symmetry, the three lowest exciton levels are degenerate at the rod's aspect ratio close to 0.9. One can see in Figures 2, (c), (d), that, similar to the spheroidal case, the oscillator strength of the lowest radiative doublet $\pm 1^L$ drops to zero at this point. However, while for the spherical shape [aspect ratio 1 in Figures 1, (a),(b)] both the upper $\pm 1^U$ and the lower $\pm 1^L$ doublets are degenerate with the states 0^U and 0^L, ± 2, respectively, at the same aspect ratio (as required by the symmetry), in Figure 1, (d) these degeneracies are clearly seen to occur at different aspect ratios.

In Figure 3, (b) we show all excitonic levels resulting from the single-particle hole energy levels shown in Figure 3, (a). The results of the calculations taking into account and neglecting the direct Coulomb interaction are shown, respectively, by red solid and black dashed lines. As the exciton binding energy is larger for lower exciton states, the exciton levels originating from the two upper hole levels in Figure 3, (a) appear shifted upward. The relatively large energy gap separating these upper exciton states allows one to disregard them when considering the fine structure of the lowest excitonic multiplet, as we did for spheroidal nanocrystals.

To summarize, in this study we have compared the fine structure of the lowest excitonic multiplet in spheroidal nanocrystals and cylindrical nanorods of III−V and II−VI semiconductors. For spheroidal shapes, the treatment of a nanocrystal's nonsphericity was perturbative and was based on Migdal's theory, which restricted its applicability to nanocrystals with aspect ratios close to 1. We have demonstrated that its responsible application is not limited by introduction of a single perturbation taking care of the shape nonsphericity, but requires fine-tuning of the perturbations describing interparticle interactions which are sensitive to the shape anisotropy, such as the electron−hole long-range exchange interaction. For three-axial ellipsoids, similar corrections will cause splittings of radiative doublets. This mechanism of the radiative doublet splittings, discussed in refs.[18,21,22] and stemming from the anisotropic long-range electron−hole exchange interaction, is competing with another mechanism, described in refs.[8,9] and based on isotropic exchange interaction and valence-band (i.e., light and heavy hole) mixing. Depending on material parameters, these two competing mechanisms can lead to splittings of either the same or opposite signs. Although contributions to the splittings of the radiative doublets caused by the mechanism leading to eq 3 are negligible for CdSe and InP colloidal nanocrystals,[2,3] this competition is, in fact, behind

https://doi.org/10.1021/acs.jpclett.4c02800
J. Phys. Chem. Lett. 2024, 15, 11753−11759

recent proposals[23,24] and experimental reports[25] of fine structure splitting cancellation in InAs epitaxial quantum dots.

Despite its restrictions, in many cases Migdal's theory is capable of producing analytical results[4,5,8,9] and is very robust and convenient. Our treatment of cylindrical nanocrystals was free of any restrictions on the cylinder's aspect ratio but involved rather tedious numerical calculations. Yet, when compared, Figures 1, 2, (a), (b) and Figures 1, 2, (c), (d), obtained, respectively, for spheroidal and cylindrical zincblende CdSe nanocrystals with the circular cross-section of radius R = 30 Å and various aspect ratios, demonstrate very similar qualitative behaviors. Thus, it appears that, in some cases, the treatment based on Migdal's theory can be used beyond its formal limits of validity, at least for a qualitative analysis.

For spheroidal nanocrystals, the degeneracy between "light" and "heavy" holes occurs for the spherical shape and is, therefore, dictated by the symmetry. For cylindrical shapes, this degeneracy is rather accidental. As a result, the role of direct electron−hole Coulomb interaction is different in the two models. For cylinders, the light- and heavy-hole excitons have slightly different binding energies and, therefore, the degeneracy point between light- and heavy-hole exciton levels (when the exchange interaction is neglected) can be shifted (if the direct Coulomb is strong enough) with respect to the degeneracy point between energy levels of the confined light and heavy holes. For the same reason, the direct Coulomb interaction affects splittings between sublevels of the lowest excitonic multiplet in cylindrical nanocrystals [cf. Figure 3, (b)]. For spheroids, the degeneracy point occurs for the spherical shape whether we take the direct Coulomb interaction into account or not. This interaction merely shifts the "center of gravity" of the multiplet without affecting the splittings between its sublevels.

The approach based on Migdal's theory assumes that the fine structure of the lowest excitonic multiplet is only affected by the four lowest spin states of the confined hole, which might not always be the case. Our treatment of cylindrical nanocrystals is more flexible in this respect.

We have tested the model of a cylindrical box for the structures with aspect ratios close to 1, where the traditional perturbative model based on Migdal's theory is valid. However, the former model should unveil its potential for nanorods which were defined in a recent review[26] as having aspect ratios from 2 to 50.

Finally, we should note that Migdal's approach can be employed to address in-plane anisotropy of cylindrical disks or rods within our treatment.

We believe that insights into exciton fine structure offered by the comparison of the two models presented here are relevant to both colloidal and epitaxial quantum dots.

■ ASSOCIATED CONTENT

Supporting Information

The Supporting Information is available free of charge at https://pubs.acs.org/doi/10.1021/acs.jpclett.4c02800.

Derivation of eq 3 and explicit form of H and ΔH (PDF)

■ AUTHOR INFORMATION

Corresponding Author

Serguei V. Goupalov − *Department of Physics, Jackson State University, Jackson, Mississippi 39217, United States;* orcid.org/0000-0002-4913-0792; Email: serguei.goupalov@jsums.edu

Complete contact information is available at: https://pubs.acs.org/10.1021/acs.jpclett.4c02800

Notes

The author declares no competing financial interest.

■ ACKNOWLEDGMENTS

The author wishes to thank Jennifer A. Hollingsworth for stimulating discussions and hospitality during his stay at LANL. This work was supported in part by the U.S. Department of Energy, Office of Science, Office of Workforce Development for Teachers and Scientists (WDTS), under the Visiting Faculty Program (VFP) and in part by NSF through DMR- 2100248.

■ REFERENCES

(1) Fernée, M. J.; Tamarat, P.; Lounis, B. Spectroscopy of single nanocrystals. *Chem. Soc. Rev.* **2014**, *43*, 1311−1337.

(2) Sinito, C.; Fernée, M. J.; Goupalov, S. V.; Mulvaney, P.; Tamarat, P.; Lounis, B. Tailoring the Exciton Fine Structure of Cadmium Selenide Nanocrystals with Shape Anisotropy and Magnetic Field. *ACS Nano* **2014**, *8*, 11651−11656.

(3) Prin, E.; Xia, C.; Won, Y.-H.; Jang, E.; Goupalov, S. V.; Tamarat, P.; Lounis, B. Revealing the Band-Edge Exciton Fine Structure of Single InP Nanocrystals. *Nano Lett.* **2023**, *23*, 6067−6072.

(4) Efros, Al.L.; Rodina, A. V. Band-edge absorption and luminescence of nonspherical nanometer-size crystals. *Phys. Rev. B* **1993**, *47*, 10005−10007.

(5) Efros, Al.L; Rosen, M.; Kuno, M.; Nirmal, M.; Norris, D. J.; Bawendi, M. Band-edge exciton in quantum dots of semiconductors with a degenerate valence band: Dark and bright exciton states. *Phys. Rev. B* **1996**, *54*, 4843−4856.

(6) Fernée, M. J.; Tamarat, P.; Lounis, B. Cryogenic Single-Nanocrystal Spectroscopy: Reading the Spectral Fingerprint of Individual CdSe Quantum Dots. *J. Phys. Chem. Lett.* **2013**, *4*, 609−618.

(7) Brodu, A.; Chandrasekaran, V.; Scarpelli, L.; Buhot, J.; Masia, F.; Ballottin, M. V.; Severijnen, M.; Tessier, M. D.; Dupont, D.; Rabouw, F. T.; Christianen, P. C. M.; de Mello Donega, C.; Vanmaekelbergh, D.; Langbein, W.; Hens, Z. Fine Structure of Nearly Isotropic Bright Excitons in InP/ZnSe Colloidal Quantum Dots. *J. Phys. Chem. Lett.* **2019**, *10*, 5468−5475.

(8) Goupalov, S. V. Effect of shape anisotropy in nanocrystals of semiconductors with small spin−orbit splitting. *J. Chem. Phys.* **2024**, *160*, 114703.

(9) Goupalov, S. V. Anisotropy-induced exchange splitting of exciton radiative doublet in CdSe nanocrystals. *Phys. Rev. B* **2006**, *74*, 113305.

(10) Migdal, A. B. *Qualitative Methods in Quantum Theory*; W.A. Benjamin: 1977.

(11) Landau, L. D.; Lifshitz, E. M. *Quantum Mechanics. Non-Relativistic Theory*, 3rd ed.; Pergamon Press: 1977.

(12) Moszkowski, S. A. Particle States in Spheroidal Nuclei. *Phys. Rev.* **1955**, *99*, 803−809.

(13) Goupalov, S. V. Effect of finite spin-orbit splitting on the electron-hole exchange interaction in excitons confined in semiconductor nanocrystals. *Phys. Rev. B* **2023**, *108*, 235419.

(14) Sercel, P. C.; Vahala, K. J. Analytical formalism for determining quantum-wire and quantum-dot band structure in the multiband envelope-function approximation. *Phys. Rev. B* **1990**, *42*, 3690−3710.

(15) Goupalov, S. V.; Ivchenko, E. L. Electron-hole long-range exchange interaction in semiconductor quantum dots. *J. Cryst. Growth* **1998**, *184* (185), 393−397.

(16) Gupalov, S. V.; Ivchenko, E. L. The Fine Structure of Excitonic Levels in CdSe Nanocrystals. *Phys. Solid State* **2000**, *42*, 2030−2038.

(17) Luttinger, J. M. Quantum Theory of Cyclotron Resonance in Semiconductors: General Theory. *Phys. Rev.* **1956**, *102*, 1030−1041.

(18) Goupalov, S. V.; Ivchenko, E. L.; Kavokin, A. V. Anisotropic exchange splitting of excitonic levels in small quantum systems. *Superlat. Microstruct.* **1998**, *23*, 1205−1209.

(19) Kiselev, V. A.; Razbirin, B. S.; Uraltsev, I. N. Additional Waves and Fabry-Perot Interference of Photoexcitons (Polaritons) in Thin II-VI Crystals. *Phys. Status Solidi B* **1975**, *72*, 161−172.
(20) Adachi, S. *Properties of group-IV, III-V and II-VI Semiconductors*; Wiley: 2005.
(21) Gupalov, S. V.; Ivchenko, E. L.; Kavokin, A. V. Fine structure of localized exciton levels in quantum wells. *J. Exp. Theor. Phys.* **1998**, *86*, 388−394.
(22) Nestoklon, M. O.; Goupalov, S. V.; Dzhioev, R. I.; Ken, O. S.; Korenev, V. L.; Kusrayev, Yu.G.; Sapega, V. F.; de Weerd, C.; Gomez, L.; Gregorkiewicz, T.; Lin, J.; Suenaga, K.; Fujiwara, Y.; Matyushkin, L. B.; Yassievich, I. N. Optical orientation and alignment of excitons in ensembles of inorganic perovskite nanocrystals. *Phys. Rev. B* **2018**, *97*, 235304.
(23) van Venrooij, N. R. S.; da Cruz, A. R.; Gajjela, R. S. R.; Koenraad, P. M.; Pryor, C. E.; Flatté, M. E. Fine structure splitting cancellation in highly asymmetric InAs/InP droplet epitaxy quantum dots. *Phys. Rev. B* **2024**, *109*, No. L201405.
(24) Zieliński, M. Vanishing fine structure splitting in highly asymmetric InAs/InP quantum dots without wetting layer. *Sci. Rep.* **2020**, *10*, 13542.
(25) Lin, C.-H.; You, W.-T.; Chou, H.-Y.; Cheng, S.-J.; Lin, S.-D.; Chang, W.-H. Anticorrelation between the splitting and polarization of the exciton fine structure in single self-assembled InAs/GaAs quantum dots. *Phys. Rev. B* **2011**, *83*, No. 075317.
(26) Shulenberger, K. E.; Jilek, M. R.; Sherman, S. J.; Hohman, B. T.; Dukovic, G. Electronic Structure and Excited State Dynamics of Cadmium Chalcogenide Nanorods. *Chem. Rev.* **2023**, *123*, 3852−3903.

https://doi.org/10.1021/acs.jpclett.4c02800
J. Phys. Chem. Lett. 2024, 15, 11753−11759